

# Integration of NOMA with Reflecting Intelligent Surfaces: A Multi-cell Optimization with SIC Decoding Errors

Wali Ullah Khan, Eva Lagunas, Zain Ali, Symeon Chatzinotas, and Björn Ottersten, *Fellow, IEEE*

**Abstract**—Reflecting intelligent surfaces (RIS) has recently emerged as one of the promising technologies for achieving high energy and spectral efficiency in next-generation wireless networks. By using low-cost passive reflecting elements, RIS can smartly reconfigure the signal propagation to extend the wireless communication coverage. On the other side, Non-orthogonal multiple access (NOMA) has been proved as a key air interface technique for supporting massive connections over limited resources. This letter proposes a new optimization framework for the multi-cell RIS-NOMA network. In particular, we address the system spectral efficiency maximization with successive interference cancellation (SIC) decoding errors. The closed-form expressions of transmit power at the base station and power allocation coefficients of users are derived using Karush–Kuhn–Tucker conditions. Moreover, an efficient reflection matrix for RIS in each cell is designed using successive convex approximation and DC programming. Simulation results are provided to demonstrate the benefits of the proposed optimization in the multi-cell RIS-NOMA network.

**Index Terms**—Reflecting intelligent surfaces (RIS), Non-orthogonal multiple access (NOMA), imperfect SIC.

## I. INTRODUCTION

THE NEXT-GENERATION wireless technologies must provide high energy and spectral efficiency to support massive connectivity [1]. In this regard, reflecting intelligent surfaces (RIS) [2] and non-orthogonal multiple access (NOMA) [3] are promising technologies. RIS can smartly reconfigure the wireless signal between transmitter and receiver using the passive elements. According to its working principle, RIS modifies the amplitude and phase of the reflective signal. By using this amazing feature, RIS can significantly enhance the performance of wireless communication in terms of coverage extension, user fairness, and channel secrecy [4]. On the other hand, NOMA has proved to be one of the key air interface techniques for high spectral efficiency and massive connectivity in next-generation wireless networks. This is because NOMA can support multiple users over the single spectrum resource simultaneously, whereas orthogonal multiple access can accommodate only one user over one spectrum resource [5]. This important feature can be achieved through superposition coding and successive interference cancellation (SIC) decoding techniques.

Researchers have recently studied the integration of NOMA with RIS in multi-cell wireless networks. For example, Ni *et al.* [6] have proposed an efficient resource allocation scheme to maximize the achievable sum rate of the multi-cell RIS-NOMA network. In another study, Elhattab *et al.* [7] have investigated a sum rate maximization problem in a two-cell RIS

NOMA network. Moreover, Rezaei *et al.* [8] have provided an energy efficiency optimization scheme for the RIS-NOMA network based on successive convex approximation. Based on the existing literature, several issues in multi-cell RIS-NOMA networks still need to be addressed. First, the authors in the above studies consider simple scenarios. For instance, the work in [6] considers three-cell while the works [7], [8] consider only two-cell system models. Second, they consider only one RIS supporting all cells, which looks impractical. Third, they assume perfect SIC decoding which is challenging to obtain in such scenarios.

This letter considers a more realistic scenario to maximize the spectral efficiency of the system under imperfect SIC decoding errors. In particular, our model consists of multi-cell ( $> 3$  cells) multi-IRS, which has not been investigated to the best of our knowledge. We simultaneously optimize the transmit power of the base station (BS) and reflection matrix of RIS in each cell while guaranteeing the minimum rate of each user. We exploit Karush-Kuhn-Tucker (KKT) conditions to calculate the to calculate the close-form expression of total transmit power at BS and power allocation coefficient of users while successive convex approximation and Difference of Convex functions (DC) programming for the design of reflection matrix in each cell. Numerical results are presented to validate our proposed optimization framework. The remainder of this work is organized as follow. Section II explains system model and states channel models. Section III formulates the spectral efficiency maximization problem and provides our proposed solution. Section IV presents and discuss the numerical results while Section V concludes this letter.

## II. SYSTEM AND CHANNEL MODELS

As shown in Fig. 1, a multi-cell RIS-NOMA network is considered, where a BS in each cell serves two down-link users. The set of BSs can be denoted as  $N$  while both users and BSs are using single antenna scenario. To enhance the wireless services and system performance, we consider a RIS in each cell which consists of  $K$  passive elements. We denote the diagonal reflection matrix of RIS as  $\Theta_n = \text{diag}\{\delta_{1,n}e^{j\theta_{1,n}}, \delta_{2,n}e^{j\theta_{2,n}}, \dots, \delta_{K,n}e^{j\theta_{K,n}}\}$ , where  $\delta_{k,n} \in [0, 1]$  is the reflection amplitude and  $\theta_{k,n} \in [0, 2\pi]$  denotes the phase shift of element  $k$ . The users serve by BS  $n$  are denoted as  $i$  and  $j$ . Without loss of generality, we assume that user  $i$  is receiving signal from BS through direct link and RIS assisted link. However, user  $j$  only receive signal through RIS assisted link due to large fading, i.e., large distance and obstacles. If  $x_n$  is the superimposed signal, then the transmit signal of BS  $n$  can be represented as  $x_n = \sqrt{P_n}\alpha_{i,n}x_{i,n} + \sqrt{P_n}\alpha_{j,n}x_{j,n}$ , where  $P_n$  denotes the transmit power of BS  $n$ ,  $\alpha_{i,n}$  and  $\alpha_{j,n}$  are the power allocation coefficients while  $x_{i,n}$  and  $x_{j,n}$  represent the unit

Wali Ullah Khan, Eva Lagunas, Asad Mahmood, Symeon Chatzinotas, and Björn Ottersten are with SnT, University of Luxembourg (Emails: {waliullah.khan, eva.lagunas, symeon.chatzinotas, bjorn.ottersten}@uni.lu).

Zain Ali is with Department of Electrical and Computer Engineering, University of California, Santa Cruz, USA (email: zainalihan1@gmail.com).

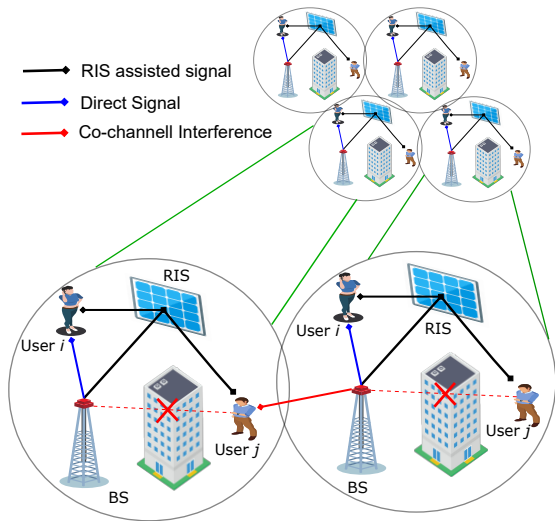


Fig. 1: System model of multi-cell RIS-NOMA network.

power signals, respectively. The received signal that user  $i$  receives from BS  $n$  through both direct and RIS assisted link can be written as:

$$y_{i,n} = \underbrace{(g_{i,n} + \mathbf{h}_{k,n} \Theta_n \mathbf{f}_{i,k,n}^H)}_{\text{desired superimposed signal}} x_n + \underbrace{\sum_{n'=1, n' \neq n}^N (g_{i,n'} + \mathbf{h}_{k,n'} \Theta_n \mathbf{f}_{i,k,n'}^H) \sqrt{P_n' \alpha_{i,n'}}}_{\text{co-channel interference from neighboring cell}} x_{i,n'} \quad (1)$$

where  $g_{i,n} = \bar{g}_{i,n} D_{i,n}^{-\eta/2}$  denotes the channel gain of direct link between BS  $n$  and user  $i$  such that  $\bar{g}_{i,n} \mathcal{CN}(0,1)$  is the Rayleigh fading coefficient and  $D_{i,n}$  shows the distance between user and BS while  $\eta$  is the path-loss exponent<sup>1</sup>. Moreover,  $\mathbf{h}_{k,n} \in K \times 1$  denotes Rician fading channels from BS  $n$  to RIS while  $\mathbf{f}_{i,k,n} \in K \times 1$  represents Rayleigh fading channels from RIS to user  $i$ . Accordingly, the received signal that user  $j$  receives through RIS assisted link can be expressed as:

$$y_{j,n} = \underbrace{\mathbf{h}_{k,n} \Theta_n \mathbf{f}_{j,k,n}^H}_{\text{desired superimposed signal}} x_n + \underbrace{\sum_{n'=1, n' \neq n}^N (g_{j,n'} + \mathbf{h}_{k,n'} \Theta_n \mathbf{f}_{j,k,n'}^H) \sqrt{P_n' \alpha_{j,n'}}}_{\text{co-channel interference from neighboring cell}} x_{j,n'} \quad (2)$$

where  $\mathbf{h}_{k,n} \in K \times 1$  denotes Rician fading channels from BS  $n$  to RIS  $m$  while  $\mathbf{f}_{j,k,n} \in K \times 1$  represents Rayleigh fading channels from RIS to user  $j$ , respectively.

Following the NOMA protocol, we assume that the user with strong channel conditions is capable of applying SIC to subtract the signal of WU before decoding its own signal. Based on the above observations, the signal to interference

plus noise ratio (SINR) of user  $i$  and user  $j$  can be computed as:

$$\gamma_{i,n} = \frac{P_n \alpha_{i,n} (|g_{i,n}|^2 + |\mathbf{h}_{k,n} \Theta_n \mathbf{f}_{i,k,n}^H|^2)}{P_n \varphi_{j,n} (|g_{i,n}|^2 + |\mathbf{h}_{k,n} \Theta_n \mathbf{f}_{i,k,n}^H|^2) \beta + I_{i,n'} + \sigma^2} \quad (3)$$

$$\gamma_{j,n} = \frac{P_n \alpha_{n,j} |\mathbf{h}_{k,n} \Theta_n \mathbf{f}_{j,k,n}^H|^2}{P_n \alpha_{i,n} |\mathbf{h}_{k,n} \Theta_n \mathbf{f}_{j,k,n}^H|^2 + I_{j,n'} + \sigma^2}, \quad (4)$$

where  $I_{i,n'} = \sum_{n'=1, n' \neq n}^N (|g_{i,n'}|^2 + |\mathbf{h}_{k,n'} \Theta_n \mathbf{f}_{i,k,n'}^H|^2) P_n' \alpha_{i,n'}$  is the co-channel interference and  $\beta$  denotes the parameter of SIC decoding error, respectively.

### III. PROBLEM FORMULATION AND PROPOSED SOLUTION

This work seeks to maximize the spectral efficiency of multi-cell RIS-NOMA network by optimizing the transmit power of BS and reflection matrix of RIS in each cell. The optimization problem can be formulated as:

$$\begin{aligned} \max_{\alpha_n, P_n, \Theta_n} & \sum_{n=1}^N \{\log_2(1 + \gamma_{i,n}) + \log_2(1 + \gamma_{j,n})\} \quad (5) \\ \text{s.t. } T_1 & : \log_2(1 + \gamma_{i,n}) \geq R_{min}, \forall n, \\ T_2 & : \log_2(1 + \gamma_{j,n}) \geq R_{min}, \forall n, \\ T_3 & : 0 \leq P_n \leq P_{tot}, \forall n, \\ T_4 & : \theta_{k,n} \in [0, 2\pi], |\delta_{k,n}| = 1, \forall k, n, \\ T_5 & : 0 \leq \alpha_{i,n} \leq 1, 0 \leq \alpha_{j,n} \leq 1, \forall n, \\ T_6 & : \alpha_{i,n} + \alpha_{j,n} = 1, \end{aligned}$$

where  $\alpha_n = \{\alpha_{i,n}, \alpha_{j,n}\}$ . The constraints  $T_1$  and  $T_2$  ensure the minimum data rate of user  $i$  and user  $j$ . Constraint  $T_3$  controls the transmit power of BS in each cell. Constraints  $T_4$  is invoked for phase shift and reflection coefficient at RIS. Constraints  $T_5$  and  $T_6$  are the power distribution restrictions of the NOMA systems.

Form the constraint  $T_6$  we have  $(a_{j,n} = 1 - a_{i,n})$ . Substituting  $(a_{j,n} = 1 - a_{i,n})$  in the the problem removes the need for  $T_6$  and also makes the problem more tractable. After the substitution, the Lagrangian of the problem is given as:

$$\begin{aligned} L = & - \sum_{n=1}^N (\log_2(1 + \gamma_{i,n}) + \log_2(1 + \gamma_{j,n})) + \sum_{n=1}^N \tau_{i,n} (R_{min} \\ & - \log_2(1 + \gamma_{i,n})) + \sum_{n=1}^N \tau_{j,n} (R_{min} - \log_2(1 + \gamma_{j,n})) + \\ & \sum_{n=1}^N \lambda_n (P_n - P_{tot}) + \sum_{k=1}^K \sum_{n=1}^N \mu_{k,n} (\theta_{k,n} - 2\pi) + \sum_{n=1}^N \\ & \eta_{i,n} (\alpha_{i,n} - 1), \quad (6) \end{aligned}$$

By adapting KKT conditions and differentiating the Lagrangian with respect to  $\alpha_{i,n}$  we get:

$$\alpha_{i,n}^6 ((\beta - 1)^2 \beta^2 \eta_{i,n} \varepsilon_i^4 \varepsilon_j^2 P_n^6) + \alpha_{i,n}^5 \Gamma_5 + \alpha_{i,n}^4 \Gamma_4 + \alpha_{i,n}^3 \Gamma_3 + \alpha_{i,n}^2 \Gamma_2 + \alpha_{i,n} \Gamma_1 + \Gamma_0 = 0, \quad (7)$$

with the values of  $\varepsilon_i$  and  $\varepsilon_j$  can be expressed as:

$$\varepsilon_i = |g_{i,n}|^2 + |\mathbf{h}_{k,n} \Theta_n \mathbf{f}_{i,k,n}^H|^2 \quad (8)$$

$$\varepsilon_j = |\mathbf{h}_{k,n} \Theta_n \mathbf{f}_{j,k,n}^H|^2 \quad (9)$$

<sup>1</sup>Other channels in the system are modeled similarly but the details are omitted here for simplicity.

and the values of  $\Gamma_0, \Gamma_1, \Gamma_2, \Gamma_3, \Gamma_4$  and  $\Gamma_5$  are given in Appendix A. The equation (7) is a polynomial of order 6 and can be easily solved by using mathematical solvers. The value of  $\alpha_{j,n}$  can be computed as  $\alpha_{j,n} = 1 - \alpha_{i,n}$ . Then differentiating with respect to  $P_n$  we get a polynomial of order 4, given as:

$$P_n^4((\alpha_{i,n} - 1)\alpha_{i,n}(\alpha_{i,n}(\beta - 1) - \beta)\beta\varepsilon_i^2\varepsilon_j^2\lambda_n) + P_n^3\Lambda_3 + P_n^2\Lambda_2 + P_n\Lambda_1 + \Lambda_0, \quad (10)$$

where  $\Lambda_0, \Lambda_1, \Lambda_2$ , and  $\Lambda_3$  are given in Appendix B. In each iteration the Lagrangian variables associated with  $\alpha_{i,n}$  and  $P_n$  are updated by using the sub-gradient method as:

$$\tau_{j,n} = \left[ \tau_{j,n} + \varpi(R_{min} - \log_2(1 + \gamma_{j,n})) \right]^+, \quad (11)$$

$$\lambda_n = \left[ \lambda_n + \varpi(P_n - P_{tot}) \right]^+, \quad (12)$$

$$\eta_{i,n} = \left[ \eta_{i,n} + \varpi(\alpha_{i,n} - 1) \right]^+, \quad (13)$$

where  $\varpi$  is the step size and  $[x]^+ = \max\{x, 0\}$ .

For finding the solution of  $\Theta_n$ , we first adopt successive convex approximation [9]. With successive convex approximation the rates of strong and WU are given as  $\zeta_{i,n} \log_2(\gamma_{i,n}) + \Omega_{i,n}$  and  $\zeta_{j,n} \log_2(\gamma_{j,n}) + \Omega_{j,n}$ , respectively. When  $\zeta_{e,n} = \frac{\gamma_{e,n}}{1 + \gamma_{e,n}}, \forall e = \{i, j\}$ , and  $\Omega_{e,n} = \log_2(1 + \gamma_{e,n}) - \frac{\gamma_{e,n}}{1 + \gamma_{e,n}} \log_2(\gamma_{e,n}), \forall e = \{i, j\}$ . Then the rates can be written as  $R_{i,n} = \zeta_{i,n}(\log_2(P_n\alpha_{i,n}(|g_{i,n}|^2 + |\mathbf{h}_{k,n}\Theta_n\mathbf{f}_{i,k,n}^H|^2)) - \log_2(P_n\alpha_{j,n}(|g_{i,n}|^2 + |\mathbf{h}_{k,n}\Theta_n\mathbf{f}_{i,k,n}^H|^2)\beta + I_{i,n'} + \sigma^2)) + \Omega_{i,n}$  and  $R_{j,n} = \zeta_{j,n}(\log_2(P_n\alpha_{n,j}|\mathbf{h}_{k,n}\Theta_n\mathbf{f}_{j,k,n}^H|^2) - \log_2(P_n\alpha_{i,n}|\mathbf{h}_{k,n}\Theta_n\mathbf{f}_{j,k,n}^H|^2 + I_{j,n'} + \sigma^2)) + \Omega_{j,n}$ . Let  $A = \Theta_n\Theta_n^H$ , where  $A \geq 0$  and  $\text{rank}(A) = 1$ . Let  $W_{i,k,n} = |\mathbf{h}_{k,n}\mathbf{f}_{i,k,n}^H|^2$ , where  $W_{i,k,n} \geq 0$  and  $\text{rank}(W_{i,k,n})=1$ . Then, for  $f_{i,1}(A) = \log_2(P_n\alpha_{i,n}(|g_{i,n}|^2 + AW_{i,k,n}))$ ,  $f_{i,2}(A) = \log_2(P_n\alpha_{j,n}(|g_{i,n}|^2 + AW_{i,k,n}\beta) + I_{i,n'} + \sigma^2)$ ,  $f_{j,1}(A) = \log_2(P_n\alpha_{j,n}(AW_{j,k,n}))$ ,  $f_{j,2}(A) = \log_2(P_n\alpha_{j,n}(|g_{j,n}|^2 + AW_{j,k,n}\beta + I_{j,n'} + \sigma^2))$ , we have:

$$\overline{R_{i,n}^*} = \zeta_{i,n}[f_{i,1}(A) - f_{i,2}(A)] + \Omega_{i,n} \quad (14)$$

$$\overline{R_{j,n}^*} = \zeta_{j,n}[f_{j,1}(A) - f_{j,2}(A)] + \Omega_{j,n} \quad (15)$$

Then employing DC programming we replace  $f_{i,2}$  and  $f_{j,2}$  with their first order linear approximation as:  $f_2(A) \leq f_2(A^{(i)}) + \text{tr}((f_2'(A^{(i)}))^H(A - A^{(i)})) = \overline{f_2(A)}$ . The optimization problem can be written as:

$$\max_A \sum_{n=1}^N (\overline{R_{i,n}^*} + \overline{R_{j,n}^*}) \quad (16)$$

$$s.t. A \geq 0, \text{diag}(A) \leq 1, \text{rank}(A) = \text{tr}(A) - \|A\|_2 = 1, \quad (17)$$

$$P_n\alpha_{i,n}(|g_{i,n}|^2 + AW_{i,k,n}) \geq \Xi(P_n\alpha_{j,n}(|g_{i,n}|^2 + AW_{i,k,n}\beta) + I_{i,n'} + \sigma^2), \forall n, \quad (18)$$

$$P_n\alpha_{j,n}AW_{j,k,n} \geq \Xi(P_n\alpha_{i,n}AW_{j,k,n}\beta + I_{i,n'} + \sigma^2), \forall n, \quad (19)$$

---

### Algorithm 1: Proposed optimization Framework

---

**Initialization:** Define all parameters of the system

**Step 1:** Compute  $\alpha_{i,n}, \alpha_{j,n}$ , and  $P_n$  for the given  $\Theta_n^*$   
**while not converge do**

**for**  $n = 1 : N$  **do**

        Compute  $\alpha_{i,n}$  using (7)

        Compute  $\alpha_{j,n}$  as  $\alpha_{j,n} = 1 - \alpha_{i,n}$

        Compute  $P_n$  using Equation (10)

        Update the dual variables in (11)–(13)

**end**

**end**

**Step 2:** Now with  $\alpha_{i,n}^*, \alpha_{j,n}^*, P_n^*$ , we compute  $\Theta_n$

**for**  $n = 1 : N$  **do**

    Find  $\Theta_n^*$  by solving the standard semi-definite programming in (20)–(23) using MOSEK toolbox of MATLAB.

**end**

Return  $\alpha_{i,n}^*, \alpha_{j,n}^*, P_n^*, \Theta_n^*$

---

$\|A\|_2$  is the spectral norm of  $A$  and  $\text{tr}(A) \sum_{n=1}^N \nu_n$  where  $\nu_n$  represents the  $n$ th largest singular value of  $A$ , and  $\Xi = 2^{R_{min}} - 1$ . Then we add the rank constraint as a penalty to the objective, with this, the optimization problem becomes:

$$\max_A \sum_{n=1}^N (\overline{R_{i,n}^*} + \overline{R_{j,n}^*}) + \xi_1(\text{tr}(A) - \|A\|_2) + \xi_1(\text{tr}(A) - \|A\|_2) \quad (20)$$

$$s.t. A \geq 0, \text{diag}(A) \leq 1, \quad (21)$$

$$P_n\alpha_{i,n}(|g_{i,n}|^2 + AW_{i,k,n}) \geq \Xi(P_n\alpha_{j,n}(|g_{i,n}|^2 + AW_{i,k,n}\beta) + I_{i,n'} + \sigma^2), \forall n, \quad (22)$$

$$P_n\alpha_{j,n}AW_{j,k,n} \geq \Xi(P_n\alpha_{i,n}AW_{j,k,n}\beta + I_{i,n'} + \sigma^2), \forall n, \quad (23)$$

where  $\|A\|_2 = \|A^{(i)}\|_2 \text{tr}(x_{max}^{(i)}(A - A^{(i)}))$ , where  $x_{max}^{(i)}$  is the eigenvector corresponding to the largest singular value of matrix  $A$  in the  $i$ th iteration. The above problem is in the form of standard semi-definite programming and is solved using MOSEK toolbox of MATLAB [10].

It is important to discuss the mathematical complexity of the proposed multi-cell RIS-NOMA optimization scheme. The complexity of the proposed scheme in any given iteration can be expressed as  $O\{2N\}$ . Now we assume that the total number iterations required for convergence are  $T$ , then the overall complexity of the proposed scheme becomes  $O\{T2N\}$ .

## IV. NUMERICAL RESULTS

Here we present the numerical results of the proposed optimization scheme. Unless mentioned otherwise, the simulation parameters are set as follows: the average channels are obtained from 10000 realizations, the power budget of each BS is 20 dBm, the number of passive elements on each RIS is 50, reuse the same carrier for all BSs, the number of users associated with each BS is 2, the path loss is 3, imperfect SIC parameter  $\beta = 0.1$ , and the variance of AWGN is set as  $\sigma^2 = 0.1$ , respectively.

To check the effect of imperfect SIC detection on the system performance, Fig. 2 plots the system spectral efficiency against

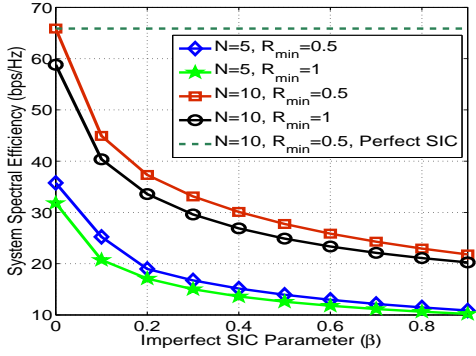


Fig. 2: The impact of imperfect SIC parameter on the Spectral efficiency of the system.

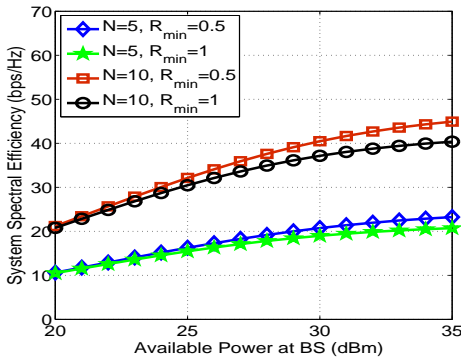


Fig. 3: The effect of increasing BS power on the system spectral efficiency with different cells and  $R_{min}$ .

the increasing values of  $\beta$  where the number of cells is set as  $J = 5$  and  $J = 10$  while the values of  $R_{min}$  is 0.5 bps/Hz and 1 bps/Hz. We can see that for all considered cases, when the value of  $\beta$  increases, the system's spectral efficiency reduces. This is because the high values of  $\beta$  increase the interference of NOMA users due to the poor signal decoding capability. Another point worth mentioning here is the decreasing spectral efficiency gap of all the cases when  $\beta$  increases. It is because with increasing  $\beta$ , more power is required by all users to meet the minimum rate requirements. Thus, the power allocation becomes less flexible. In practical systems achieving perfect SIC is a difficult task. However, for ease of solution most of the works in literature consider perfect SIC. Considering perfect SIC provides an over-optimistic performance evaluation as is shown in Fig. 2.

Next, it is important to show the impact of allocating power on the system's performance. Fig. 3 shows the increasing values of  $P_{tot}$  versus spectral efficiency of the system. The spectral efficiency increases with increasing the allocated transmit power of BS. Further, the gap in the spectral efficiency offered by all the cases also increases with  $P_{tot}$ , because more available transmit power at BS becomes available for optimization. Hence, the cases with less restrictions (smaller  $R_{min}$  requirements) perform better than other cases with higher rate requirements. Besides that, we can see that the system spectral efficiency similarly increases as the number of cells increases from 5 to 10. It shows the effectiveness of

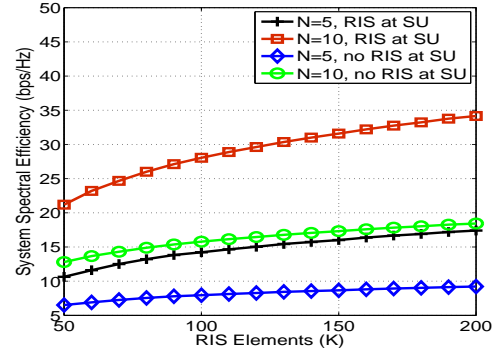


Fig. 4: This figure shows the effect of increasing RIS elements on the System Spectral Efficiency.

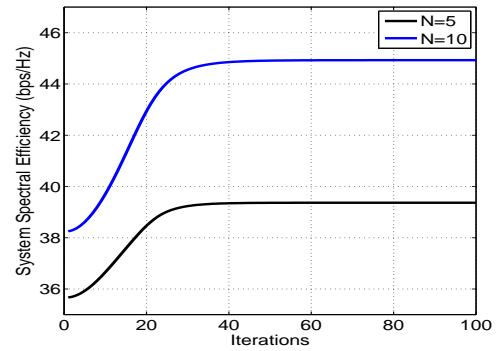


Fig. 5: Convergence of System Spectral Efficiency.

the proposed scheme for a large RIS-NOMA network.

Fig. 4 shows the impact of increasing number of RIS elements on the spectral efficiency of the system. We have compared the performance of the considered system model with a scenario where the RIS forwards the signal of only WU in each cell. Whereas, the strong user (SU) only receives its signal directly from the BS. As expected, increasing RIS elements increases the spectral efficiency of the system for any number of cells for both cases. Further, it can be seen that we get much better performance when the RIS forwards the data of both SU and WU in the cell. All the results in this section showed that the systems with more number of cells provide better spectral efficiency of the system. This shows the importance of the proposed scheme in the large-scale multi-cell RIS-NOMA networks. Fig. 5 show the convergence behavior of the proposed framework. It can be seen from the figure that the system converges within reasonable number of iterations, and that increasing the number of interfering cells has little impact on the convergence time.

## V. CONCLUSIONS

The integration of NOMA with RIS has the potential to extend wireless communication and connect massive devices in next-generation networks. This letter has proposed a new optimization scheme for a multi-cell RIS-NOMA network to maximize the system's spectral efficiency. Specifically, our framework simultaneously optimizes the transmit power of

BS and the reflection matrix of RIS in each cell under SIC decoding errors. The total transmit power of BS and power allocation coefficients of users have been calculated using KKT conditions, while the efficient reflection matrix of RIS has been designed by successive convex approximation and DC programming. Simulation results have confirmed the benefits of the proposed optimization scheme.

#### APPENDIX A: VALUES OF $\Gamma_0, \Gamma_1, \Gamma_2, \Gamma_3, \Gamma_4$ AND $\Gamma_5$

$$\Gamma_0 = (I_{j,n'} + \sigma^2)(I_{i,n'} + \beta\varepsilon_i P_n + \sigma^2)^3 (\eta_{i,n}(I_{j,n'} + \sigma^2) (I_{i,n'} + \beta\varepsilon_i P_n + \sigma^2) + P_n(-\varepsilon_i(I_{j,n'} + \sigma^2)(1 + \tau_{i,n}) + \varepsilon_i(I_{i,n'} + \beta\varepsilon_i P_n + \sigma^2)(1 + \tau_{j,n})))$$

$$\Gamma_1 = P_n(I_{i,n'} + \beta(\varepsilon_i P_n + \sigma^2))^2 (2\eta_{i,n}(I_{j,n'} + \sigma^2)(I_{i,n'} + \beta(\varepsilon_i P_n + \sigma^2))(-2\beta - 1)(\varepsilon_i(I_{j,n'} + \sigma^2) + \varepsilon_j)(I_{i,n'} + \beta(\varepsilon_i P_n + \sigma^2)) + P_n((2\beta - 1)(\varepsilon_i)^2(I_{j,n'} + \sigma^2)^2(1 + \tau_{i,n}) + (\varepsilon_j)^2(I_{i,n'} + \beta(\varepsilon_i P_n + \sigma^2))^2(1 + \tau_{j,n}) - 2(\varepsilon_i)\varepsilon_j(I_{j,n'} + \sigma^2)(I_{i,n'} + \beta(\varepsilon_i P_n + \sigma^2)(\tau_{i,n} - \tau_{j,n} + 2\beta(1 + \tau_{j,n}))))$$

$$\Gamma_2 = P_n^2(I_{i,n'} + \beta\varepsilon_i P_n + \sigma^2)(\eta_{i,n}(I_{i,n'} + \beta\varepsilon_i P_n + \sigma^2))((1 + 6(\beta - 1)\beta)\varepsilon_i^2(I_{j,n'} + \sigma^2)^2 - 4(2\beta - 1)\varepsilon_i\varepsilon_j(I_{j,n'} + \sigma^2)(I_{i,n'} + \beta\varepsilon_i P_n + \sigma^2) + \varepsilon_j^2(I_{i,n'} + \beta\varepsilon_i P_n + \sigma^2)^2) - \varepsilon_i P_n((\beta - 1)\beta\varepsilon_i^2(I_{j,n'} + \sigma^2)^2(1 + \tau_{i,n}) + \varepsilon_j^2(I_{i,n'} + \beta\varepsilon_i P_n + \sigma^2)^2(\tau_{i,n} - 1 - 2\tau_{j,n} + 4\beta(1 + \tau_{j,n})) - \varepsilon_i\varepsilon_j(I_{j,n'} + \sigma^2)(I_{i,n'} + \beta\varepsilon_i P_n + \sigma^2)(-1 - 2\tau_{i,n} + \tau_{j,n} + 2\beta(3\beta - 1 + 2\tau_{i,n} + 3(\beta - 1)\tau_{j,n}))))$$

$$\Gamma_3 = -\varepsilon_i P_n^3(I_{i,n'} + \beta\varepsilon_i P_n + \sigma^2)(2\eta_{i,n}((\beta - 1)\beta(2\beta - 1)\varepsilon_i^2(I_{j,n'} + \sigma^2)^2 - (1 + 6(\beta - 1)\beta\varepsilon_i\varepsilon_j(I_{j,n'} + \sigma^2)(I_{i,n'} + \beta\varepsilon_i P_n + \sigma^2) + (2\beta - 1)\varepsilon_j^2(I_{i,n'} + \beta\varepsilon_i P_n + \sigma^2)^2) - \varepsilon_i\varepsilon_j P_n(-2\beta^3\varepsilon_i(2I_{j,n'} - 3\varepsilon_j P_n + 2\sigma^2)(1 + \tau_{j,n}) + \varepsilon_j(I_{i,n'} + \sigma^2)(\tau_{j,n} - \tau_{i,n}) + \varepsilon_j(2I_{i,n'}(\tau_{i,n} - 2 - 3\tau_{j,n}) + 2\sigma^2(\tau_{i,n} - 2 - 3\tau_{j,n})\varepsilon_i P_n(\tau_{j,n} - \tau_{i,n}))) + 2\beta^2 + (-\varepsilon_i(I_{j,n'} + \sigma^2)(\tau_{i,n} - 2 - 3\tau_{j,n}) + \varepsilon_j(3\sigma^2 + \varepsilon_i P_n + (\tau_{i,n} - 2) + 3(I_{i,n'} + (I_{i,n'} - \varepsilon_i P_n + \sigma^2)\tau_{j,n}))))$$

$$\Gamma_4 = \varepsilon_i^2 P_n^4(\eta_{i,n}((\beta - 1)^2\beta^2\varepsilon_i^2(I_{j,n'} + \sigma^2)^2 - 4(\beta - 1)\beta(2\beta - 1)\varepsilon_i\varepsilon_j(I_{j,n'} + \sigma^2)(I_{i,n'} + \beta\varepsilon_i P_n + \sigma^2) + (1 + 6(\beta - 1)\beta)\varepsilon_j^2(I_{i,n'} + \beta\varepsilon_i P_n + \sigma^2)^2) - (\beta - 1)\beta\varepsilon_i\varepsilon_j P_n(-1(\beta - 1)\beta\varepsilon_i(I_{j,n'} + \sigma^2)(1 + \tau_{j,n}) + \varepsilon_j(I_{i,n'} + \beta\varepsilon_i P_n + \sigma^2)(\tau_{i,n} - 1 - 2\tau_{j,n} + 4\beta(1 + \tau_{j,n}))))$$

$$\Gamma_5 = (\beta - 1)\beta\varepsilon_i^3\varepsilon_j P_n^5(2\eta_{i,n}(-(\beta - 1)\beta\varepsilon_i(I_{j,n'} + \sigma^2) + (2\beta - 1)\varepsilon_j(I_{i,n'} + \beta\varepsilon_i P_n + \sigma^2)) + (\beta - 1)\beta\varepsilon_i\varepsilon_j P_n(1 + \tau_{j,n}))$$

#### APPENDIX B: VALUES OF $\Lambda_0, \Lambda_1, \Lambda_2$ AND $\Lambda_3$

$$\Lambda_0 = (I_{i,n'} + \sigma^2)(I_{j,n'} + \sigma^2)(-I_{j,n'} + \sigma^2)(-\lambda_n(I_{i,n'} + \sigma^2) + \alpha_{i,n}\varepsilon_i(1 + \tau_{i,n})) + (\alpha_{i,n} - 1)\varepsilon_j(I_{i,n'} + \sigma^2)(1 + \tau_{j,n}))$$

$$\Lambda_1 = (I_{i,n'} + \sigma^2)(I_{j,n'} + \sigma^2)(\varepsilon_j\lambda_n(I_{i,n'} + \sigma^2) - \alpha_{i,n}^2\varepsilon_i\varepsilon_j(\tau_{i,n} - \tau_{j,n} + 2\beta(1 + \tau_{j,n})) - 2\beta\varepsilon_i(-\lambda_n(I_{j,n'} + \sigma^2) + \varepsilon_j(1 + \tau_{j,n})) + \alpha_{i,n}(\varepsilon_j\lambda_n(I_{i,n'} + \sigma^2) + |g_{i,n}|^2(-2\beta - 1)\lambda_n(\varepsilon_j + \sigma^2) - \varepsilon_j(2 + \tau_{i,n} + \tau_{j,n} - 4\beta(1 + \tau_{j,n}))) + |\mathbf{h}_{k,n}\mathbf{\Theta}_n\mathbf{f}_{i,k,n}^H|^2(-2\beta - 1)\lambda_n(I_{j,n'} + \sigma^2) - \varepsilon_j(2 + \tau_{i,n} + \tau_{j,n} - 4\beta(1 + \tau_{j,n}))))$$

$$\Lambda_2 = \alpha_{i,n}^3(\beta - 1)\beta\varepsilon_i^2\varepsilon_j(I_{j,n'} + \sigma^2)(1 + \tau_{j,n}) + \beta\varepsilon_i(I_{j,n'} + \sigma^2)(2\varepsilon_j\lambda_n(I_{i,n'} + \sigma^2) - \beta\varepsilon_j(\lambda_n(\varepsilon_j + \sigma^2) + \varepsilon_j(1 + \tau_{j,n}))) + \alpha_{i,n}(\varepsilon_j\lambda_n(I_{i,n'} + \sigma^2)(\varepsilon_j(I_{i,n'} + \sigma^2) + \varepsilon_i(I_{j,n'} + \sigma^2)) + \beta\varepsilon_i^2(I_{j,n'} + \sigma^2)(\lambda_n(I_{j,n'} + \sigma^2) - \varepsilon_j(1 + \tau_{j,n})) + \beta^2\varepsilon_i^2(I_{j,n'} + \sigma^2)(-2\lambda_n(I_{j,n'} + \sigma^2) + 3\varepsilon_j(1 + \tau_{j,n}))) - \alpha_{i,n}^2\varepsilon_i(-(\beta - 1)\beta\varepsilon_i\lambda_n(\varepsilon_j + \sigma^2)^2 + \varepsilon_j^2(I_{i,n'} + \sigma^2)(1 + \tau_{i,n}) + \varepsilon_j(I_{j,n'} + \sigma^2)(1 + \tau_{i,n}) + \varepsilon_j(I_{j,n'} + \sigma^2)(-\lambda_n(I_{i,n'} + \sigma^2) + 3\beta^3\varepsilon_i(1 + \tau_{j,n}) - 2\beta(\varepsilon_i - \lambda_n(I_{i,n'} + \sigma^2) + \varepsilon_i\tau_{j,n})))$$

$$\Lambda_3 = \varepsilon_i\varepsilon_j\lambda_n(\alpha_{i,n}^3(\beta - 1)\beta\varepsilon_i(I_{j,n'} + \sigma^2) + \beta^2\varepsilon_i(I_{j,n'} + \sigma^2) + \alpha_{i,n}\beta(2\varepsilon_j(I_{i,n'} + \sigma^2) - (\beta - 1)\varepsilon_i(I_{j,n'} + \sigma^2)) - \alpha_{i,n}^2((2\beta - 1)\varepsilon_j(I_{i,n'} + \sigma^2) + \beta^2\varepsilon_i(I_{j,n'} + \sigma^2)))$$

#### REFERENCES

- [1] M. Giordani *et al.*, "Toward 6G networks: Use cases and technologies," *IEEE Commun. Mag.*, vol. 58, no. 3, pp. 55–61, Mar. 2020.
- [2] S. Gong *et al.*, "Toward smart wireless communications via intelligent reflecting surfaces: A contemporary survey," *IEEE Commun. Surveys Tut.*, vol. 22, no. 4, pp. 2283–2314, 2020.
- [3] W. U. Khan *et al.*, "NOMA-enabled optimization framework for next-generation small-cell IoV networks under imperfect SIC decoding," *IEEE Trans. Intelligent Transportation Systems*, pp. 1–10, 2021.
- [4] —, "Opportunities for physical layer security in UAV communication enhanced with intelligent reflective surfaces," *arXiv preprint arXiv:2203.16907*, 2022.
- [5] L. Dai *et al.*, "A survey of non-orthogonal multiple access for 5G," *IEEE Commun. Surveys Tut.*, vol. 20, no. 3, pp. 2294–2323, 2018.
- [6] W. Ni *et al.*, "Resource allocation for multi-cell IRS-aided NOMA networks," *IEEE Trans. Wireless Commun.*, vol. 20, no. 7, pp. 4253–4268, July 2021.
- [7] M. Elhattab *et al.*, "RIS-assisted joint transmission in a two-cell downlink NOMA cellular system," *IEEE J. Selected Areas Commun.*, vol. 40, no. 4, pp. 1270–1286, April 2022.
- [8] A. Rezaei *et al.*, "Energy-efficient resource allocation and antenna selection for IRS-assisted multi-cell downlink networks," *IEEE Wireless Commun. Lett.*, pp. 1–1, 2022.
- [9] J. Papandriopoulos and J. S. Evans, "SCALE: A low-complexity distributed protocol for spectrum balancing in multiuser DSL networks," *IEEE Trans. Information Theory*, vol. 55, no. 8, pp. 3711–3724, 2009.
- [10] J. Zuo *et al.*, "Resource allocation in intelligent reflecting surface assisted NOMA systems," *IEEE Trans. Commun.*, vol. 68, no. 11, pp. 7170–7183, 2020.